nature biomedical engineering

ARTICLES

https://doi.org/10.1038/s41551-020-0555-4

Check for updates

A co-formulation of supramolecularly stabilized insulin and pramlintide enhances mealtime glucagon suppression in diabetic pigs

Caitlin L. Maikawa[1], Anton A. A. Smith[2,3], Lei Zou[4], Gillie A. Roth[1], Emily C. Gale[5], Lyndsay M. Stapleton[1], Sam W. Baker[6], Joseph L. Mann[2], Anthony C. Yu[2], Santiago Correa[2], Abigail K. Grosskopf[7], Celine S. Liong[1], Catherine M. Meis[2], Doreen Chan[8], Megan Troxell[9], David M. Maahs[10,11], Bruce A. Buckingham[10,11], Matthew J. Webber[4] and Eric A. Appel[1,2,10,11] ✉

Treatment of patients with diabetes with insulin and pramlintide (an amylin analogue) is more effective than treatment with insulin only. However, because mixtures of insulin and pramlintide are unstable and have to be injected separately, amylin analogues are only used by 1.5% of people with diabetes needing rapid-acting insulin. Here, we show that the supramolecular modification of insulin and pramlintide with cucurbit[7]uril-conjugated polyethylene glycol improves the pharmacokinetics of the dual-hormone therapy and enhances postprandial glucagon suppression in diabetic pigs. The co-formulation is stable for over 100 h at 37 °C under continuous agitation, whereas commercial formulations of insulin analogues aggregate after 10 h under similar conditions. In diabetic rats, the administration of the stabilized co-formulation increased the area-of-overlap ratio of the pharmacokinetic curves of pramlintide and insulin from 0.4 ± 0.2 to 0.7 ± 0.1 (mean ± s.d.) for the separate administration of the hormones. The co-administration of supramolecularly stabilized insulin and pramlintide better mimics the endogenous kinetics of co-secreted insulin and amylin, and holds promise as a dual-hormone replacement therapy.

There are over 422 million people living with diabetes worldwide and 5–10% of these people have type 1 diabetes[1]. These patients often suffer from severe side effects, such as renal failure, heart disease, vision loss and limb amputation, which can all be prevented with tight glycaemic control. Type 1 diabetes occurs after an autoimmune response resulting in the destruction of pancreatic β cells responsible for the production and secretion of metabolically active hormones including insulin and amylin. Patients with type 1 diabetes are therefore unable to produce the insulin required for glucose uptake by cells. Amylin complements the action of insulin to regulate blood glucose levels by acting centrally to slow gastric emptying, suppress postprandial glucagon secretion and decrease food intake by increasing satiety (Fig. 1a)[2–10]. Similar to insulin, amylin production is insufficient at diagnosis and deteriorates with ongoing autoimmune destruction in individuals with type 1 diabetes. Furthermore, patients with type 1 diabetes experience additional loss of metabolic signalling such as suppression of postprandial glucagon secretion, resulting in glucagon-driven glycogenolysis that compounds mealtime hyperglycaemic excursions (Fig. 1a).

Insulin replacement therapy has been the focus of diabetes treatment for over 80 years, yet amylin has been largely overlooked. Current treatments use subcutaneous injections or infusion from pumps to deliver insulin. A true hormone replacement therapy for patients with type 1 diabetes would simultaneously deliver amylin and insulin. Amylin replacement therapy is critical to regain suppression of postprandial glucagon, which cannot be achieved with subcutaneous insulin delivery alone (Fig. 1 and Supplementary Fig. 1). Amylin replacement therapy has proven to be challenging because amylin is highly unstable in formulation and rapidly aggregates into amyloid fibrils[11], prompting the development of the amylin analogue pramlintide, which acts through similar mechanisms to amylin in vivo. Pramlintide differs from amylin by alterations to three amino acids that suppress amyloid fibrillation and enable its stable formulation at about pH 4 (refs. [2–9]). Unfortunately, insulin and its analogues are typically formulated at approximately pH 7.4, which means that insulin and pramlintide must be administered in two separate injections. Patients treated with a combination of insulin and pramlintide at mealtimes have been shown to have improved glycaemic control, observed as a 0.3% decrease in HbA1c levels in comparison to patients treated with insulin alone[4,5,7,8,12–14]. Despite the increased efficacy of dual-hormone treatment, by 2012 only 29,000 patients of over 2,100,000 patients who would potentially benefit from such a treatment had adopted it due to the burdensome requirement for administration as two separate injections[15].

In addition to formulation challenges, the pharmacokinetics of insulin and pramlintide in current formulations are highly dissimilar and the resulting lack of pharmacokinetic overlap does not mimic their natural mode of action. In healthy individuals, insulin and amylin are co-secreted at a fixed ratio from the β-cells in the pancreas and act with similar kinetics[16]. In contrast, the current

[1]Department of Bioengineering, Stanford University, Stanford, CA, USA. [2]Department of Materials Science and Engineering, Stanford University, Stanford, CA, USA. [3]Department of Science and Technology, Aarhus University, Aarhus, Denmark. [4]Department of Chemical and Biomolecular Engineering, University of Notre Dame, Notre Dame, IN, USA. [5]Department of Biochemistry, Stanford University, Stanford, CA, USA. [6]Department of Comparative Medicine, Stanford University, Stanford, CA, USA. [7]Department of Chemical Engineering, Stanford University, Stanford, CA, USA. [8]Department of Chemistry, Stanford University, Stanford, CA, USA. [9]Department of Pathology, Stanford University, Stanford, CA, USA. [10]Department of Pediatrics (Endocrinology), Stanford University, Stanford, CA, USA. [11]Diabetes Research Center, Stanford University, Stanford, CA, USA. ✉e-mail: eappel@stanford.edu

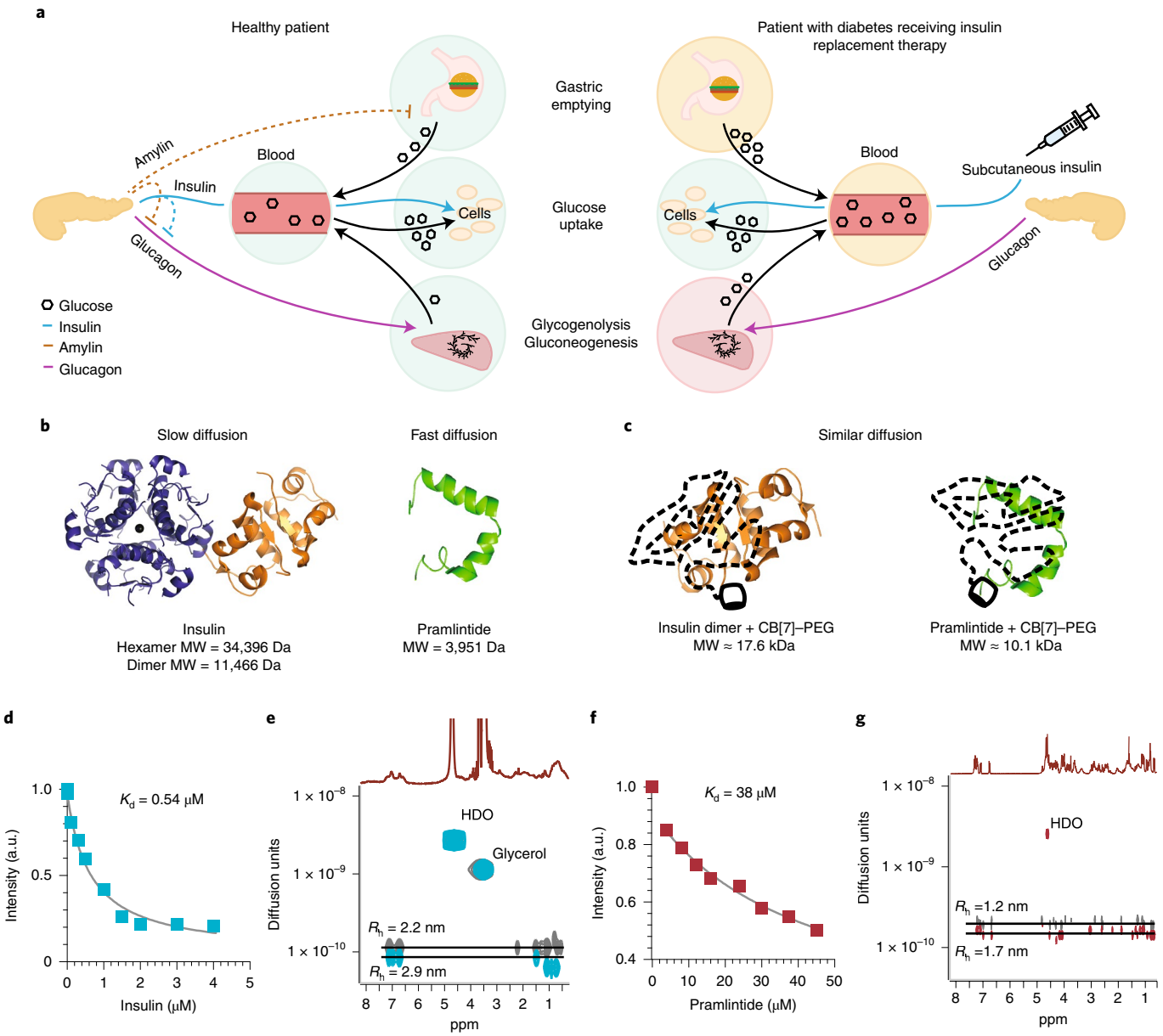

Fig. 1 | CB[7]–PEG binds to insulin and pramlintide and alters diffusion rates in formulation. a, Schematic of post-mealtime metabolic signalling pathways in healthy individuals (left) and patients with type 1 diabetes who are receiving insulin replacement therapy (right). In healthy individuals, endogenous insulin promotes cellular glucose uptake and acts with amylin to locally suppress postprandial glucagon, thus decreasing glycogenolysis and gluconeogenesis. In contrast, treatment of patients with diabetes with subcutaneous insulin alone cannot restore glucagon suppression. Amylin replacement is critical to fully restore metabolic signalling and constitute a true hormone replacement therapy. **b**,**c**, Schematics demonstrating how molecular weight affects diffusion rates, which directly impact the absorption kinetics following subcutaneous administration. **b**, Standard insulin formulations comprise a mixture of insulin aggregation states (that is, hexamers and dimers) that exhibit an extended duration of insulin action when injected into the subcutaneous space. In contrast, the pramlintide monomer is rapidly absorbed into the blood. **c**, Following complexation with CB[7]–PEG such that only insulin dimers exist in the formulation, insulin and pramlintide have molecular weights and diffusion rates that are more similar to one another. **d**,**f**, Acridine orange competitive binding assay for aspart (**d**; $n=1$ experiment) and pramlintide (**f**, $n=1$ experiment), indicating binding of CB[7] to both proteins. **e**,**g**, DOSY NMR provides insight into the formation of protein–CB[7]–PEG complexes and their rates of diffusion in formulation. In these studies, the aspart–CB[7]–PEG complex (**e**, cyan) exhibits a 30% reduction in the diffusion rate compared with standard dimeric aspart (grey). Moreover, the pramlintide–CB[7]–PEG complex (**g**, red) exhibits an approximately twofold reduction in the diffusion rate compared with pramlintide alone (grey). Complexation of the two proteins with CB[7]–PEG results in a ratio of the diffusion rates of pramlintide–CB[7]–PEG to aspart–CB[7]–PEG of only 1.6 compared with 2.3 for pramlintide and aspart in typical formulations, indicating that the diffusivities of the proteins are more similar in co-formulation. MW, molecular weight; a.u., arbitrary units; HDO, hydrogen deuterium oxide from water; horizontal black lines highlight individual compounds and their diffusivities.

'rapid-acting' insulin analogue formulations Humalog (insulin lispro) and Novolog (insulin aspart) exhibit a delayed onset of action of approximately 20–30 min, peak action at about 60–90 min and total duration of action of about 3–4 h (refs. [4,6,17,18]), whereas Symlin (pramlintide) begins to act almost immediately, exhibits a peak action at about 20 min and total duration of action of approximately

90 min. This large dissimilarity in pharmacokinetics arises from the distinct aggregation states of the proteins in the formulation and the resulting impact on absorption behaviour. These insulin formulations contain a mixture of hexamers, dimers and monomers, which dissociate following subcutaneous injection and are absorbed at different rates, resulting in the delayed onset and long duration of action of these formulations (Fig. 1b)[19–21]. In contrast, the pramlintide monomer is absorbed rapidly from the subcutaneous space (Fig. 1b). The lack of overlap between the insulin and pramlintide pharmacokinetics in current treatment strategies hinders the synergistic effects of pramlintide and insulin action. Recent clinical studies have moved towards evaluating the benefits of delivering a fixed ratio of insulin and pramlintide using two separate pumps to better simulate endogenous insulin–pramlintide secretion[22–24]. Although the use of two separate pumps can deliver a fixed ratio of pramlintide to insulin[24], this method is overly burdensome outside of a research setting and does not address the poor pharmacokinetic overlap of these two hormones following subcutaneous administration.

A new class of excipients are needed for protein formulation to address the concerns surrounding aggregation and denaturation over time[25,26]. Covalent PEGylation has been successful as a strategy to stabilize insulin and amylin in formulation[27–29]; however, covalent modification of proteins often interferes with their activity, typically extends their pharmacokinetics in vivo and can lead to increased immunogenicity[30]. Recent research has shown that non-covalent modification of proteins can enhance their stability in formulation[31,32]. In particular, cucurbit[*n*]urils (CB[*n*]) are a family of macrocyclic hosts that exhibit strong binding affinities for aromatic amino acids[33–36] and have a reassuring safety profile[37–39]. The conjugation of a polyethylene glycol (PEG) chain to CB[7] creates a designer excipient (CB[7]–PEG) for non-covalent PEGylation of protein therapeutics. Insulin has an amino (N)-terminal phenylalanine and pramlintide has an amidated carboxy (C)-terminal tyrosine, making them ideal targets for supramolecular modification using the CB[7]–PEG system[31]. In this work, we exploit CB[7]–PEG for simultaneous supramolecular PEGylation of insulin and pramlintide to stabilize the two hormones in a co-formulation whereby the therapeutic ratio is defined in the formulation. We demonstrate that this dual-hormone therapy can be administered as a single injection, thus reducing burden, and that the increased overlap between the pharmacokinetics of the two pharmaceuticals restores postprandial glucagon suppression in a swine model of insulin-deficient diabetes for tighter glycaemic control and enhanced diabetes management.

Results

Characterization of CB[7]–PEG binding. CB[7]–PEG with varying PEG molecular weights has been shown to bind to recombinant human insulin with micromolar affinities, increasing its stability in formulation and enabling simple tuning of the duration of insulin action in a mouse model of insulin-deficient diabetes through modulation of the PEG molecular weight[31]. In this study, we chose to work with CB[7]–PEG_{5k} because of its demonstrated capacity to stabilize recombinant human insulin in formulation without significantly extending the insulin duration of action in vivo. We aimed to stabilize insulin and pramlintide together in formulation as well as use co-formulation as an opportunity to simultaneously alter the pharmacokinetics of the two hormones in vivo to more closely match one another. Through a combination of insulin hexamer disruption by removal of the formulation zinc and simultaneous complexation of insulin and pramlintide with CB[7]–PEG, the effective hydrodynamic size of both components become similar to one another (Fig. 1b,c). We hypothesized that this similarity in hydrodynamic size, which directly impacts absorption following subcutaneous administration, would promote a greater overlap between the pharmacokinetic profiles of the two therapeutics.

We evaluated an insulin analogue, aspart, because it is the active ingredient in the most commonly used commercial rapid-acting insulin formulation Novolog. We determined the binding affinity of CB[7] to both aspart and pramlintide using a competitive binding assay with acridine orange (AO; Fig. 1d,f). The binding of CB[7] to aspart was determined to be 0.54 μM, which is similar to values previously reported for binding to recombinant insulin[31], whereas the binding to pramlintide was determined to be 38 μM. The higher binding affinity of CB[7] to insulin compared with pramlintide is due to the well-documented higher binding affinity of CB[7] to N-terminal aromatic amino acids on account of the hydrophobic guest being flanked by a protonated amine group[31]. Circular dichroism confirmed that the binding of both aspart and pramlintide with CB[7]–PEG did not affect protein structure (See Supplementary information and Supplementary Fig. 2).

We then used diffusion-ordered NMR spectroscopy (DOSY) to provide insight into the hydrodynamic size and diffusion characteristics of the protein–CB[7]–PEG complexes (Fig. 1e,g and Supplementary Figs. 3,4). In these studies, aspart was formulated with CB[7]–PEG and EDTA to remove formulation zinc. EDTA forms strong complexes with zinc (dissociation constant (K_d)$\approx 10\times10^{-18}$ M)[40,41] and the addition of one molar equivalent of EDTA relative to the zinc found in insulin formulations rapidly sequesters the zinc, preventing it from interacting with the insulin and disrupting insulin-hexamer formation in solution. In DOSY experiments, CB[7]–PEG and aspart were found to diffuse together, thus verifying the binding interaction observed previously using competitive binding assays. The aspart dimer exhibited a diffusion rate of approximately 1.2×10^{-10} m^2 s^{-1}, whereas the complex of aspart–CB[7]–PEG exhibited a 30% lower diffusion rate of approximately 8.7×10^{-11} m^2 s^{-1}. The Stokes–Einstein relationship specifies that the diffusion rate is inversely proportional to the size of the species in solution, whereby a 50% increase in the molecular weight is expected to decrease the diffusion rate by roughly one-third, as observed in this study. We used this relationship to approximate the hydrodynamic radius (R_h) to be 2.2 nm for dimeric aspart and 2.9 nm for the aspart–CB[7]–PEG complex. For comparison, the insulin hexamer has an R_h of approximately 2.8 nm (ref. [42]).

Similarly, the diffusion rate for pramlintide decreased from 2×10^{-10} m^2 s^{-1} for the protein alone to 1.4×10^{-10} m^2 s^{-1} for the pramlintide–CB[7]–PEG complex, corresponding to a change in R_h from 1.2 nm to 1.7 nm. The degree of diffusion-rate increase after the addition of CB[7]–PEG to pramlintide was lower than that observed for aspart, probably due to the weaker and more dynamic binding. We observed that the ratio of the diffusion rates of the pramlintide–CB[7]–PEG and aspart–CB[7]–PEG complexes was approximately 1.6, whereas the ratio of the diffusion rates for pramlintide alone and insulin in a standard formulation was approximately 2.3. These observations suggest that the zinc-free co-formulation of the two protein–CB[7]–PEG complexes makes the two hormones more similar in hydrodynamic size than is possible with standard formulation approaches.

Formulation stability in vitro. To determine whether CB[7]–PEG stabilizes pramlintide in combination with insulin at physiological pH, the aggregation of insulin and pramlintide over time under stressed conditions (37 °C with continuous agitation) was assessed. As insulin and pramlintide destabilize, they form amyloid fibrils, which are insoluble, inactive and often immunogenic[43–45]. These aggregates are large and scatter light, and thus the degree of aggregation can be evaluated by measuring the change in transmittance over time[31].

Commercial Novolog and Humalog both aggregate in these stressed ageing conditions after 10 ± 1 and 6 ± 0.2 h, respectively, but are both stabilized for over 100 h when formulated with CB[7]–PEG (See Supplementary information and Supplementary Fig. 5).

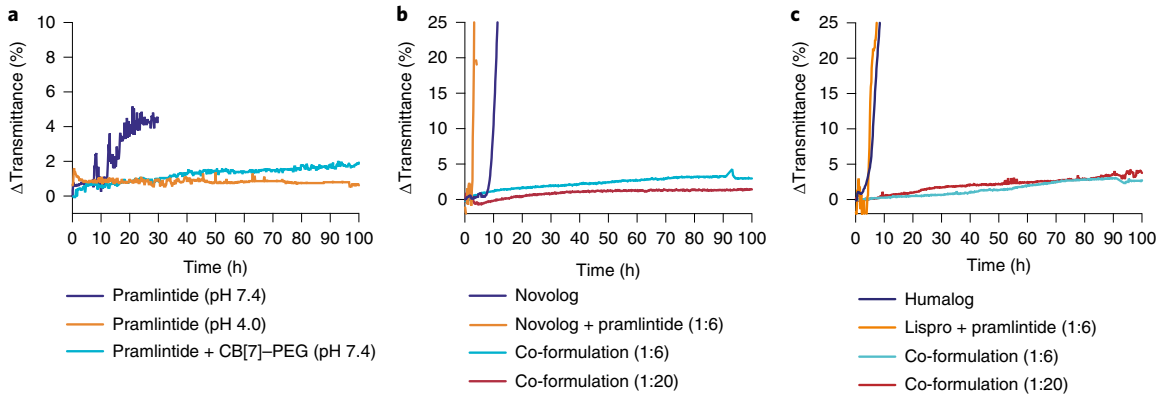

Fig. 2 | Formulation with CB[7]–PEG stabilizes a co-formulation of pramlintide and Novolog or Humalog at physiological pH. a, In vitro stability of pramlintide formulations at various pH values with and without CB[7]–PEG. **b**, In vitro stability of pramlintide–aspart (molar ratios of 1:6 and 1:20) co-formulations with CB[7]–PEG at physiological pH. **c**, In vitro stability of pramlintide–lispro (molar ratios of 1:6 and 1:20) co-formulations with CB[7]–PEG at physiological pH. The co-formulations were compared with controls of commercial Novolog or Humalog and mixtures of the incompatible aspart + pramlintide or lispro + pramlintide in the absence of CB[7]–PEG. These assays assess the aggregation of proteins over time in formulation during stressed ageing (that is, continuous agitation at 37 °C) by monitoring the changes in transmittance at 540 nm. These experiments demonstrate that a formulation with CB[7]–PEG prevents protein aggregation over the 100-h period assayed, even when commercial formulations aggregate within 10 h. The data shown are average transmittance traces for $n = 3$ samples per group.

Pramlintide formulated in sodium acetate buffer (pH 4; similar to the commercial formulation Symlin) was stable for over 100 h under stressed conditions (Fig. 2a); however, when formulated in PBS (pH 7.4), pramlintide aggregated after only 15 ± 4 h, indicating a dramatic reduction in stability at physiological pH. In contrast, when formulated with CB[7]–PEG in PBS (pH 7.4), pramlintide remained stable for over 100 h under stressed conditions.

In addition to stabilizing pramlintide and insulin analogues separately, CB[7]–PEG facilitated the development of a stable insulin–pramlintide co-formulation (Fig. 2b,c). Pramlintide co-formulated with either aspart or lispro in PBS (pH 7.4) in the absence of CB[7]–PEG aggregated after only 2.9 ± 0.2 (aspart + pramlintide) or 4.9 ± 0.3 h (lispro + pramlintide) under stressed conditions, whereas co-formulation with CB[7]–PEG in the same buffer conditions was completely stable for the duration of the 100-h kinetic study. These results demonstrate that simultaneous supramolecular PEGylation of pramlintide with either aspart or lispro and CB[7]–PEG enables the development of a viable dual-hormone co-formulation.

Pharmacodynamics and pharmacokinetics in diabetic rats. Having established the stability of the insulin–pramlintide co-formulation, we evaluated our co-formulation in vivo by measuring the blood glucose as well as the insulin and pramlintide pharmacokinetics in a well-studied rat model of insulin-deficient diabetes[46]. We hypothesized that an increase in the overlap between the insulin and pramlintide pharmacokinetics will enable the development of a more physiologically relevant dual-hormone treatment. Here, Novolog refers to the administration of the available commercial formulation, whereas insulin aspart formulations contain isolated zinc-free insulin aspart. In these studies, aspart–pramlintide co-formulations (PBS at pH 7) comprising zinc-free aspart (1.5 U kg^{-1}), CB[7]–PEG (five equivalents relative to insulin) and pramlintide (1:15, 1:8 or 1:2 equivalents relative to insulin) were compared with commercial Novolog alone (1.5 U kg^{-1}) and the clinically relevant combination of Novolog (1.5 U kg^{-1}) and pramlintide (in sodium acetate buffer, pH 4) administered as separate injections (Fig. 3a–c). The rationale of the pramlintide concentrations used is discussed in the Supplementary information.

The rate of blood glucose depletion following administration in fasted diabetic rats was similar for all treatment groups and a blood glucose drop from 448 ± 17 (time (t) = 0) to 116 ± 17 mg dl^{-1} (t = 60 min) was observed across all treatment groups. The molar ratio of pramlintide to Novolog had no effect on the rate or degree of blood glucose depletion.

Serum concentrations of insulin and pramlintide over time following the subcutaneous administration of each of the treatments outlined above were measured by ELISA to assess the degree of overlap between the pharmacokinetic profiles of the two hormones. The area under the curve (AUC) of aspart following administration in co-formulation with pramlintide (10 ± 6 mU ml^{-1}) was significantly lower than when administered alone in commercial Novolog (29 ± 8 mU ml^{-1}; t = 4.47 (where t refers to the t-statistic); degree of freedom (df) = 10; 95% confidence interval (CI) (−27,203, −9,099); P = 0.0012; Fig. 3e). These results suggest that pramlintide affects the serum concentrations of aspart and that this effect is amplified when the dual-hormone therapy is administered in a co-formulation treatment rather than as two separate injections (See Supplementary information). The 'onset' rate of fast-acting insulins is often determined using two metrics: (1) time to 50% of the normalized peak height up and (2) time to peak insulin serum concentration. Normalized serum concentration data were used to compare the time to peak aspart concentrations between treatment groups (Fig. 3h). No difference was observed in either measures for aspart following the administration of commercial Novolog alone, Novolog alongside a separate injection of pramlintide or administration in a single co-formulation injection (Fig. 3i,j). There was also no significant difference in the duration of action of aspart, determined by measuring the terminal time to 50% of the normalized peak height, between treatment groups (Fig. 3k).

When the pramlintide pharmacokinetics were evaluated, no significant differences were observed in pramlintide AUC following different treatments (Fig. 3f,g). No significant differences were seen in the pramlintide time-to-onset or peak action when pramlintide and insulin were administered as separate injections compared with the insulin–pramlintide co-formulation (Fig. 3m,n). In contrast, the duration of action of pramlintide was extended from 17 ± 3 min for separate administrations to 21 ± 4 min for the co-formulation (t = 2.26; df = 10; 95% CI (0.07, 9.065); P = 0.047; Fig. 3o). As hypothesized, an extended pramlintide duration of action resulted in an increase in overlap between the aspart and pramlintide pharmacokinetics (t = 4.01; df = 10; 95% CI (0.15, 0.52); P = 0.0025). The overlap of the pharmacokinetic profiles can be represented by the

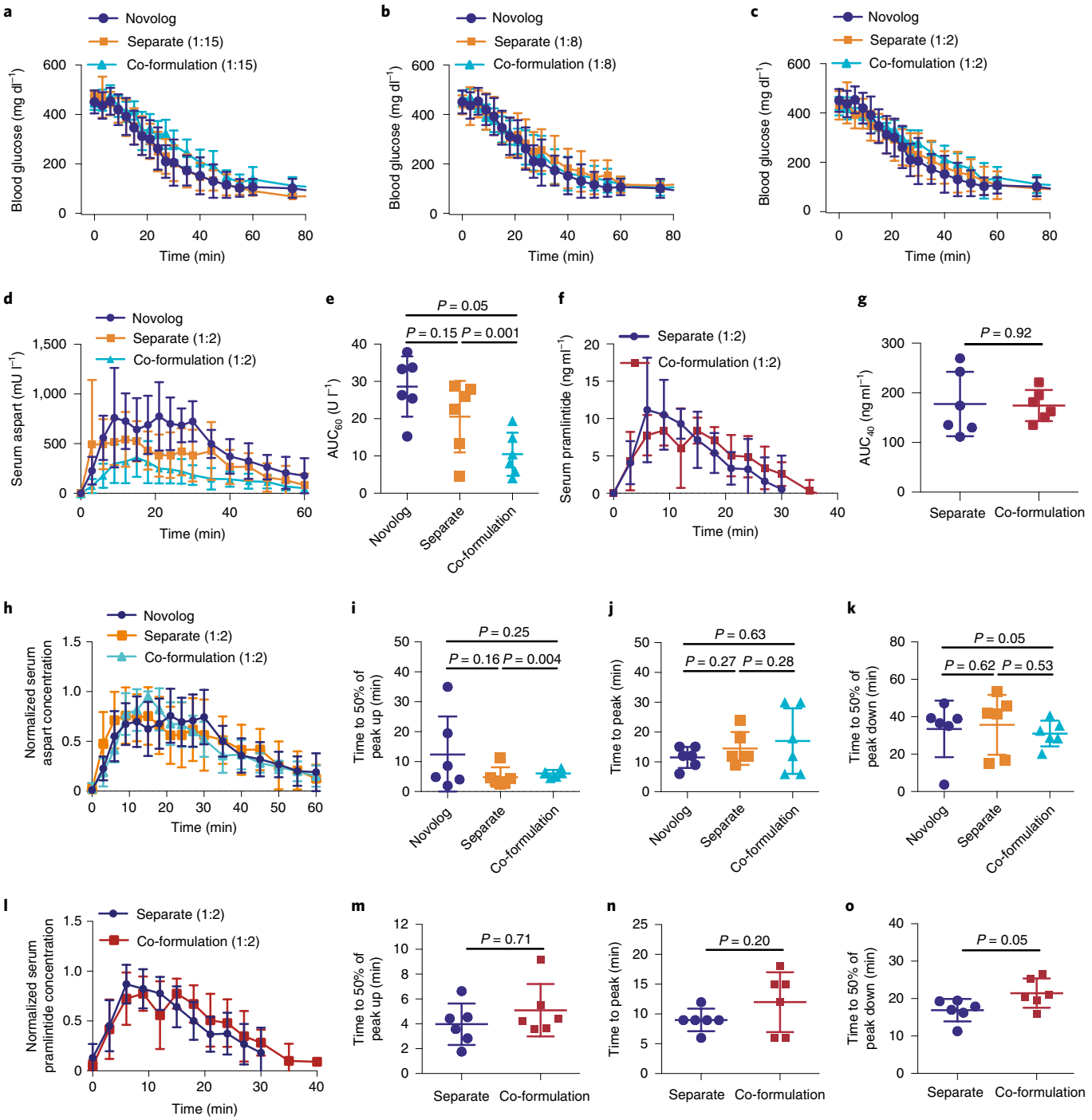

Fig. 3 | Aspart and pramlintide pharmacokinetics following different administration routes in diabetic rats. Diabetic male rats ($n = 6$) that had been fasted received subcutaneous administration of therapies comprising commercial Novolog, commercial Novolog and pramlintide (pH 4) delivered with separate injections or an aspart–pramlintide co-formulation with CB[7]–PEG. All treatment groups received 1.5 U kg^{-1} insulin. **a**–**c**, The blood glucose levels at ratios of 1:15 (**a**), 1:8 (**b**) and 1:2 (**c**) pramlintide to aspart were evaluated. All pharmacokinetic studies were evaluated with pramlintide at a ratio of 1:2 aspart to pramlintide. **d**,**f**, Pharmacokinetics of insulin aspart (**d**) or pramlintide (**f**). **e**,**g**, The AUC of the pharmacokinetic curves for aspart and pramlintide (**g**) for the first 60 min or 40 min, respectively, after subcutaneous injection. **h**,**l**, The pharmacokinetics for each rat were individually normalized to the peak serum levels and the normalized values were averaged for the aspart (**h**) and pramlintide (**l**) concentrations of each treatment group. **i**,**m**, Time to reach 50% of the peak serum concentrations of aspart (**i**) and pramlintide (**m**; onset). **j**,**n**, Time to reach peak aspart (**j**) and pramlintide (**n**) serum concentrations. **k**,**o**, Time for the depletion of 50% of the peak serum concentrations of aspart (**k**) and pramlintide. The mean ± s.d. is shown for $n = 6$ animals in all groups. Statistical significance was determined using a two-tailed Student's *t*-test.

ratio of AUC of serum pramlintide to aspart, which increased from 0.4 ± 0.2 when these proteins were delivered separately to 0.7 ± 0.1 when delivered in co-formulation (Fig. 4).

Pharmacodynamics and pharmacokinetics in diabetic pigs. We conducted studies in a swine model of insulin-deficient diabetes to assess the translationally relevant pharmacokinetics and

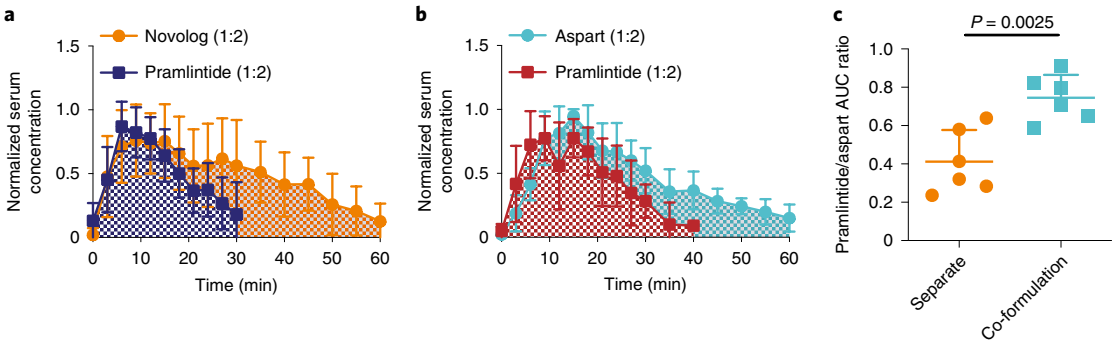

Fig. 4 | Administration of aspart and pramlintide as a co-formulation in diabetic rats enhances the pharmacokinetic overlap. a,**b**, Mean normalized serum concentration (normalized for each rat) of Novolog and pramlintide when administered as two separate injections (**a**) or a pramlintide–aspart co-formulation with CB[7]–PEG at physiological pH (**b**). **c**, Ratio of the AUC of the pharmacokinetic profiles of pramlintide and aspart administered as separate injections and as a co-formulation. The mean ± s.d. is shown for $n = 6$ animals per group. Statistical significance was determined using a two-tailed Student's *t*-test.

postprandial treatment benefits (See Supplementary information) of insulin–pramlintide co-formulations. Fasted diabetic swine were initially treated with commercial Humalog (4 U; 0.13 U kg^{-1}), separate injections of commercial Humalog (4 U; 0.13 U kg^{-1}) and pramlintide (pH 4; pramlintide:insulin, 1:6) or lispro–pramlintide co-formulation (4 U insulin; pramlintide:insulin, 1:6; CB[7]–PEG:lispro + pramlintide molar ratio, 3:1; Supplementary Fig. 7). Although the pigs that received a meal but no insulin showed the expected increase in blood glucose levels, no difference in blood glucose was observed between each of the formulations tested and no postprandial glucose excursions were observed in the treated groups (Supplementary Fig. 6). The serum or plasma concentrations of lispro and pramlintide over time following a meal given simultaneously with the subcutaneous administration of the different treatments outlined above were then measured by ELISA (Fig. 5). When delivered as a part of the co-formulation, the AUC of the lispro pharmacokinetic curve was lower than when delivered as a separate injection from insulin. Consistent with the data for rats, no differences were observed in the lispro time-to-onset, peak action or duration of action between the treatment groups (Fig. 5e–h). Pramlintide pharmacokinetics demonstrated increased time-to-onset ($t = 2.53$; df = 24; 95% CI (0.67, 6.55); $P = 0.018$) and prolonged duration of action ($t = 2.53$; df = 24; 95% CI (2.06, 20.47); $P = 0.019$) when administered as a part of the co-formulation (onset, 9 ± 3 min; duration, 58 ± 7 min) compared with administration as a separate injection (onset, 6 ± 4 min; duration, 47 ± 14 min; Fig. 5i–l). These observations corroborate the observations of the pharmacokinetics of pramlintide made in rats. The modulation of the pramlintide pharmacokinetics was confirmed by an increase in the overlap between the pharmacokinetic curves of insulin and pramlintide when administered as a co-formulation compared with when administered as separate injections (Fig. 6a–c). The ratio of the overlap time to the total time at half-peak height was determined to be 0.67 ± 0.29 for the co-formulation and 0.42 ± 0.30 for the separate injections ($t = 2.15$; df = 24; 95% CI (0.010, 0.487); $P = 0.042$).

We hypothesized that an increase in the overlap between the pharmacokinetics of insulin and pramlintide in our insulin–pramlintide co-formulation would be advantageous for the treatment outcomes. The co-formulation resulted in suppressed postprandial glucagon levels (1 ± 16 pM) compared with both Humalog alone (14 ± 16 pM; $t = 2.09$; df = 25; 95% CI (−25.39, −0.21); $P = 0.0465$) as well as insulin and pramlintide delivered as two separate injections (14 ± 17 pM; $t = 2.06$; df = 26; 95% CI (−25.13, −0.03); $P = 0.0495$; Fig. 6d,e). Separate injections did not result in statistically significant differences in postprandial glucagon suppression compared with Humalog alone ($t = 0.04$; df = 25; 95% CI (−12.97, 12.53); $P = 0.97$). These results suggest that co-formulation improves the restoration of metabolic signalling compared with the separate delivery of insulin and pramlintide.

Biocompatibility of CB[7]–PEG. As CB[7]–PEG is a new chemical entity, we sought to assess its biocompatibility using blood chemistry and histopathology to look for potential negative effects on the liver or kidney. Healthy Sprague Dawley rats ($n = 4$) were given daily injections of CB[7]–PEG (at a dose equivalent to what would be administered in an insulin injection) for 6 weeks. Their blood chemistry was monitored biweekly and single-blinded assessment of the histopathology of the liver and kidneys was conducted at the endpoint of the study (See Supplementary information and Supplementary Fig. 8). No differences were observed between the treated animals and untreated controls during these studies. The blood chemistry of diabetic pigs that received intermittent injections of the insulin–pramlintide co-formulation (1:6) containing CB[7]–PEG corroborated the findings in rats (Supplementary Fig. 9).

Discussion

Natural insulin secretion results in insulin levels that are several times higher in the liver than in the peripheral tissues as a result of first-pass insulin absorption from the portal vein. Although subcutaneous insulin replacement therapy successfully stimulates glucose uptake in the peripheral tissues, it does not suppress hepatic glucose secretion to the same degree as endogenous insulin due to differential pharmacokinetics, pharmacodynamics and biodistribution. In turn, the reduction in hepatic signalling results in unrestricted glycogen mobilization in the postprandial period. A physiological replacement therapy for amylin in diabetic patients may play an important role in improving the efficacy of insulin treatments, given that amylin and its analogues act synergistically to inhibit glycogen mobilization from hepatic tissues by suppressing postprandial glucagon[47]. However, co-formulation of biopharmaceuticals is difficult because of their poor stability and potential for differential solubility, and traditional formulation approaches to prepare an insulin–pramlintide co-formulation have been unsuccessful.

In this study, a co-formulation of insulin and pramlintide was created using an approach that utilizes simultaneous supramolecular PEGylation of the two hormones with CB[7]–PEG to stabilize pramlintide in combination with insulin analogues such as aspart or lispro in the absence of formulation zinc. We demonstrated the utility of this simple excipient-based approach to simultaneously

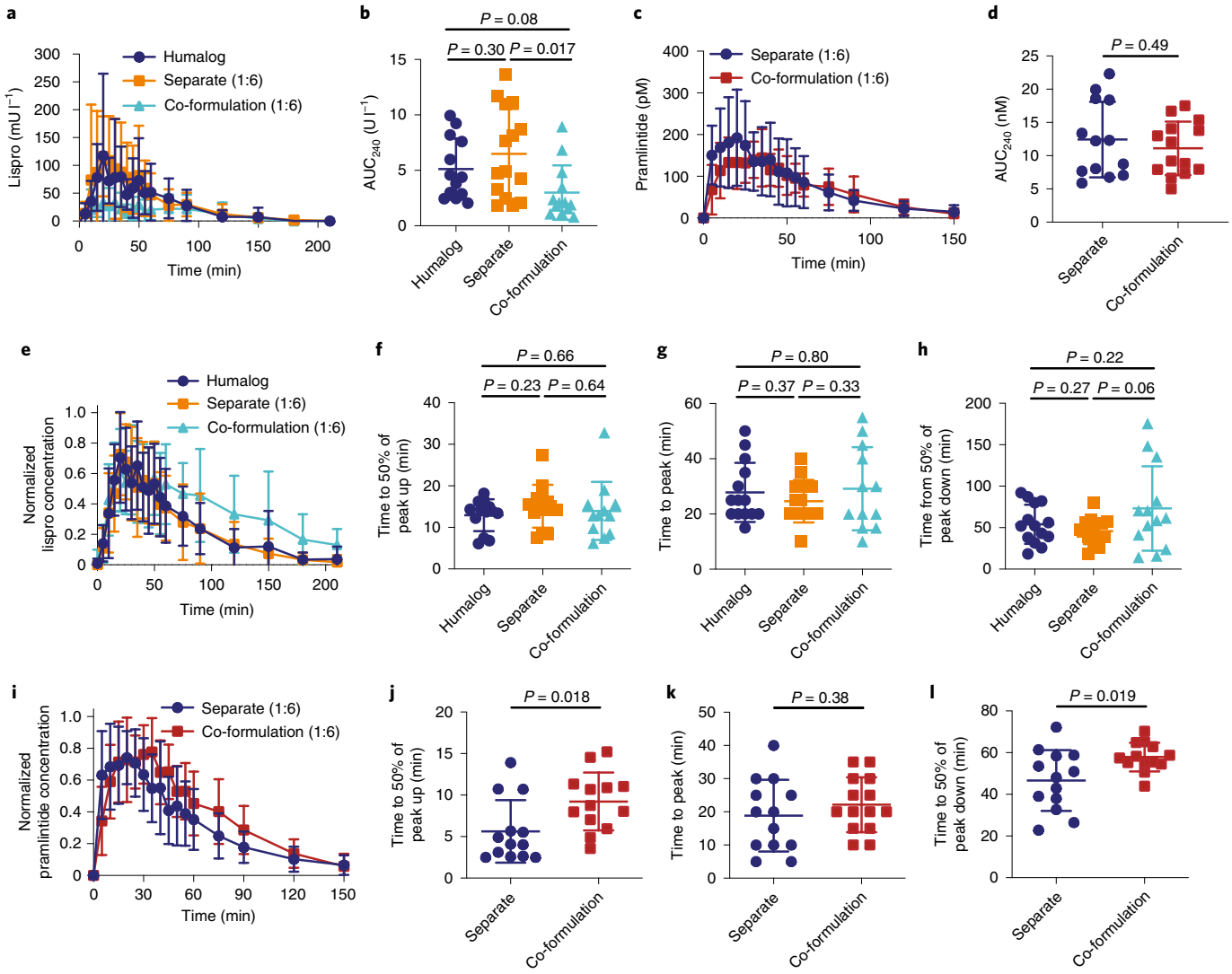

Fig. 5 | Lispro and pramlintide pharmacokinetics following different administration routes in diabetic pigs. Diabetic female pigs received subcutaneous administration of therapies comprising commercial Humalog, commercial Humalog and pramlintide (pH 4) delivered as separate injections or a lispro–pramlintide co-formulation with CB[7]–PEG. The treatments were administered simultaneously with a 200 g meal. All treatment groups received 4 U insulin and the pramlintide groups received a molar ratio of 1:6 pramlintide to lispro. **a**,**c**, Pharmacokinetics of insulin lispro (**a**; Humalog, $n=14$; separate, $n=15$; co-formulation, $n=13$) and pramlintide (**c**; $n=14$ for both groups). **b**,**d**, AUC of the pharmacokinetic curves of lispro (**b**; Humalog, $n=12$; separate, $n=14$; co-formulation, $n=13$) and pramlintide (**d**; separate, $n=13$; co-formulation, $n=14$) for the first 240 min after subcutaneous injection. **e**,**i**, The pharmacokinetics for each pig were individually normalized to the peak concentrations, and the normalized values were averaged for the lispro (**e**; Humalog, $n=14$; separate, $n=15$; co-formulation, $n=13$) and pramlintide (**i**; $n=14$ for both groups) concentration of each treatment group. **f**,**j**, Time to reach 50% of the peak lispro (**f**; Humalog, $n=13$; separate, $n=14$; co-formulation, $n=12$) and pramlintide (**j**; onset; $n=13$ for both groups) concentrations. **g**,**k**, Time to reach peak lispro (**g**; Humalog and separate, $n=14$; co-formulation, $n=12$) and pramlintide (**k**; separate, $n=13$; co-formulation, $n=14$) concentrations. **h**,**l**, Time to the depletion to 50% of the peak concentrations of lispro (**h**; Humalog, $n=14$; separate, $n=15$; co-formulation, $n=13$) and pramlintide (**l**; $n=13$ for both groups). The mean ± s.d. is shown. The Grubbs' outlier test ($\alpha=0.05$) was used to remove outliers. Statistical significance was determined using a two-tailed Student's *t*-test.

endow the otherwise incompatible proteins insulin and pramlintide with PEG chains to inhibit protein aggregation[31]. This approach exploits the specific and strong binding of the macrocyclic host molecule CB[7] to aromatic amino acids—including the N-terminal phenylalanine on insulin and the amidated C-terminal tyrosine on pramlintide[33–36]—through simple mixing, as these interactions are non-covalent. CB[7]–PEG exhibits binding affinities for these proteins in the micromolar range such that over 98% of the complexes are bound at typical formulation concentrations, yet fewer than 1% are bound on dilution, following administration in the body. This feature affords the automatic release of authentic unmodified therapeutic proteins following administration and overcomes the limitations of traditional approaches to covalent grafting of polymers onto proteins, which include reduced activity[28,48]. This approach thereby offers a broadly useful and modular excipient strategy for the formulation of unmodified protein drugs to enhance their formulation shelf life and alter pharmacokinetics.

We hypothesized that simultaneous supramolecular PEGylation of insulin and pramlintide would not only enable their co-formulation at physiological pH by enhancing the stability of the two proteins but would also facilitate the modification of the insulin–pramlintide pharmacokinetics to more closely mimic endogenous hormone

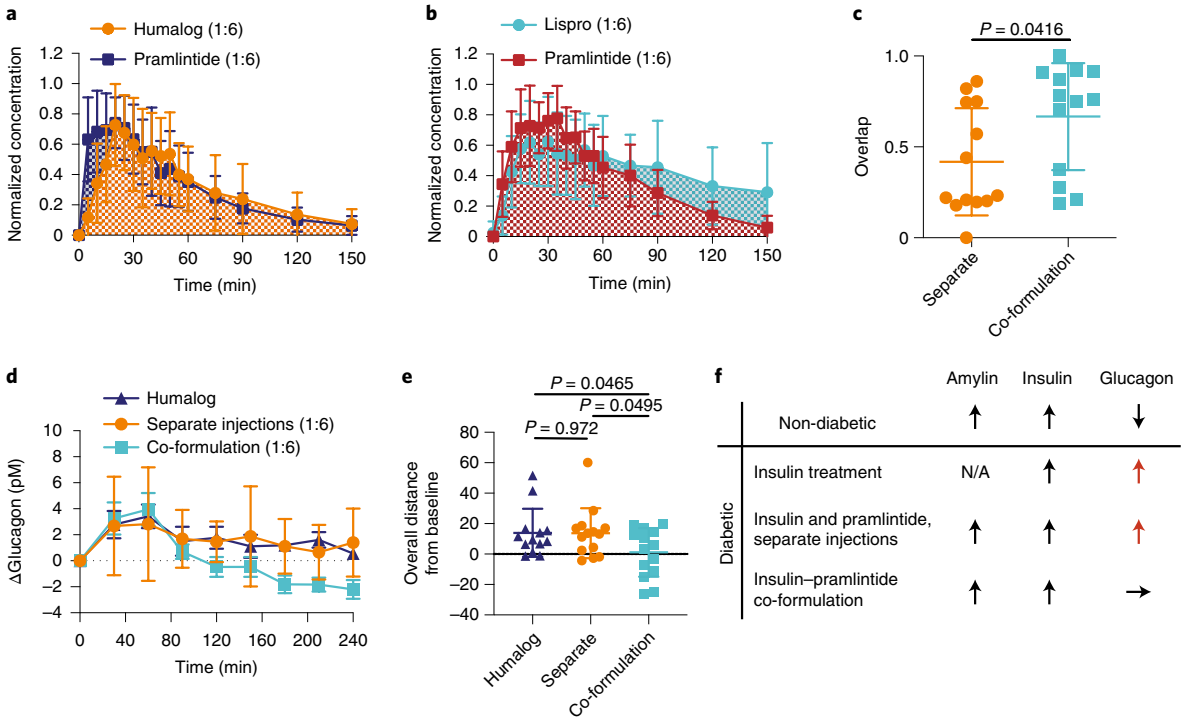

Fig. 6 | Overlap between the pharmacokinetic curves of lispro and pramlintide, and glucagon suppression following the treatment of diabetic pigs with different formulations. a–**c**, Pharmacokinetics of lispro and pramlintide after injection with Humalog and pramlintide as separate injections and as a lispro–pramlintide co-formulation. **a**,**b**, Mean normalized concentration (normalized individually for each pig) of lispro and pramlintide when administered as two separate injections (**a**; Humalog, $n=15$; pramlintide, $n=13$) or as a co-formulation (**b**; Lispro, $n=13$; pramlintide, $n=14$) with CB[7]-PEG. **c**, The overlap between the curves was evaluated as the time during which both the lispro and pramlintide concentrations were greater than 0.5 (width at half-peak height), shown as a ratio of the overlap time to the total width of both peaks (overlap ÷ (lispro + pramlintide − overlap); $n=13$ for both groups). **d**,**e**, Pharmacokinetics of glucagon after a meal and treatment with Humalog alone, Humalog and pramlintide as separate injections or as a lispro–pramlintide co-formulation. **d**, Glucagon plotted as the change in glucagon concentrations from the baseline (dotted line) over 4 h following treatment administration. **e**, Overall distance from baseline of the different treatment groups (sum of individual points; Humalog, $n=13$; separate and co-formulation, $n=14$). The co-formulation reduced glucagon levels compared with Humalog as well as separate administrations of Humalog and pramlintide. **f**, Summary schematic of how treatment affects postprandial glucagon. The black arrows denote the restoration of protein secretion to be similar to that of healthy individuals, while the red arrows denote protein secretion that differs from the endogenous response of healthy individuals. N/A, not applicable. The specified sample size n refers to a cohort of 11 pigs that received each treatment an equal number of times. The mean ± s.d. are shown. The ROUT test ($Q=1\%$) was used to remove outliers. Statistical significance was determined using a two-tailed Student's t-test.

secretion and restore mealtime glucagon suppression. When injected separately according to the current clinical model, fast-acting insulin analogues and pramlintide have a reduced overlap between their pharmacokinetic curves resulting from the slower absorption of traditionally formulated insulin (that is, consisting of a combination of monomers, dimers and hexamers) from the subcutaneous space than the pramlintide, which only exists in a monomeric form. Using a translationally relevant porcine model of insulin-deficient diabetes, we demonstrated that the mealtime administration of an insulin–pramlintide co-formulation leads to increased overlap between the insulin and pramlintide pharmacokinetics and the restoration of mealtime glucagon suppression compared with the clinical standard of separate administration of the hormones. Although the separate delivery of pramlintide has been clinically shown to suppress mealtime glucagon at high doses, we show that an insulin–amylin co-formulation exhibits potent glucagon suppression at lower doses than what can be achieved with separate administrations. Co-formulation therefore captures the synergistic effects of amylin and insulin and shows promise as a true biomimetic dual-hormone replacement therapy with greater physiological relevance than insulin alone. Moreover, the ability to administer this biomimetic dual-hormone treatment therapy in a single injection will reduce patient burden and potentially enable a broader adoption by patients who would benefit from such a therapy.

Outlook

In this study we have demonstrated that simultaneous non-covalent PEGylation of insulin and pramlintide imbue enhanced stability and enable their co-formulation at physiological pH. This dual-hormone co-formulation exhibits pharmacokinetics that more closely mimic endogenous co-secretion of these two hormones from the healthy pancreas and restores postprandial glucagon suppression compared with separately delivered insulin and pramlintide. Furthermore, with the development of automated insulin delivery systems, the co-administration of insulin and amylin analogues in a single formulation could play a major role in allowing for a fully automated closed-loop system without the need for meal announcement or meal boluses[22–24]. Future studies will require comprehensive assessment of the biocompatibility and immunogenicity of CB[7]–PEG and the complete insulin–pramlintide co-formulation to facilitate the clinical translation of this co-formulation.

Methods

Materials. CB[7]–PEG was prepared according to published protocols[31], with method modifications to enable copper 'click' chemistry following reported protocols[49]. Novolog (Novo Nordisk), Humalog (Eli Lilly) and pramlintide (BioTang) were purchased and used as received. For the pig studies, lispro was isolated using PD MidiTrap G-10 gravity columns (GE Healthcare) and then concentrated using Amino Ultra 3K centrifugal units (Millipore). All other reagents were purchased from Sigma-Aldrich, unless otherwise specified.

DOSY NMR. ^{1}H NMR DOSY spectra were recorded at a protein concentration (aspart or pramlintide) of 6 mg ml^{-1} in 200 mM phosphate buffer, pH 7, in D_2O. One dimensional H^1-NMR of the complex showed a broadening of both the insulin and CB[7]–PEG signals (Supplementary Fig. 3). This was exacerbated with an increasing ratio of CB[7]–PEG to insulin (Supplementary Fig. 4). As such, an optimum ratio of CB[7]–PEG to insulin for DOSY was established to be 1.25 mol. A Varian Inova 600 MHz NMR instrument was used to acquire the data. The magnetic field strengths ranged from 2 to 57 G cm^{-1}. The DOSY time and gradient pulse were set at 132 ms (Δ) and 3 ms (δ) respectively. All NMR data were processed using MestReNova 11.0.4 software.

AO binding affinity. For these studies, unmodified CB[7] was purchased from Strem Chemicals and AO was purchased from Sigma-Aldrich. Binding of CB[7] to Novolog and pramlintide was assessed using the AO dye displacement assay as previously described[31]. Briefly, 6 μM CB[7] and 8 (Novolog assay) or 2 μM (pramlintide assay) AO were combined with 100 μl of either the Novolog or pramlintide samples. The Novolog samples were diluted to concentrations of 0, 0.01, 0.1, 0.3, 0.5, 1, 1.5, 2, 3 and 4 μM in H_2O. The pramlintide samples were diluted to concentrations of 0, 4, 8, 12, 18, 24, 30, 37.5 and 40 μM in H_2O. The samples were incubated overnight in light-free conditions and fluorescent spectra were collected on a BioTek SynergyH1 microplate reader, exciting at 485 nm and collecting the resulting fluorescent spectra from 495 to 650 nm. The decay in the peak of AO fluorescent signal was fitted to a one-site competitive binding model (GraphPad Prism, version 6.0), using the CB[7]·AO equilibrium constant reported previously ($K_{eq} = 2 \times 10^5$ M^{-1})[50] to determine the binding constants of unmodified CB[7] to insulin and pramlintide.

Circular dichroism. Circular dichroism was used to validate that binding between CB[7]–PEG insulin aspart and pramlintide resulted in no changes to the secondary structure of the protein. Novolog was diluted to 0.2 mg ml^{-1} in PBS (pH 7.4) and evaluated alone, with EDTA at a 1:1 molar ratio to zinc, with CB[7]–PEG at a 5:1 molar excess to insulin (1.1 mg ml^{-1}) and with both EDTA and CB[7]–PEG. Even under dilute formulation conditions, 93% of insulin would be bound by CB[7]-PEG. Pramlintide was evaluated both alone in PBS at 0.5 mg ml^{-1} and with an excess of CB[7]–PEG at a concentration of 1.1 mg ml^{-1}. After mixing, the samples were left to equilibrate for 15 min at room temperature. Near-ultraviolet circular dichroism spectroscopy was performed at 20 °C using a J-815 CD Spectropolarimeter (Jasco Corporation) over a wavelength range of 185–250 nm using a cell with a 0.1 cm path length.

In vitro stability. The methods used for the aggregation assays of recombinant human insulin were adapted from previous studies[31]. Briefly, formulation samples were plated at 150 μl per well ($n = 3$ per group) in a clear 96-well plate and sealed with an optically clear and thermally stable seal (VWR). The plate was immediately placed into a plate reader and incubated with continuous shaking at 37 °C. Absorbance readings were taken every 10 min at 540 nm for 100 h (BioTek SynergyH1 microplate reader). The aggregation of insulin leads to light scattering, which results in a reduction of sample transmittance. The time for aggregation was defined as a >10% increase in transmittance from the transmittance at time zero. The controls included: (1) Novolog, (2) Humalog, (3) zinc-free Novolog (1:1 EDTA), (4) zinc-free Humalog (1:1 EDTA), (5) pramlintide (in sodium acetate buffer, pH 4), (6) pramlintide (in PBS, pH 7), (7) aspart + pramlintide (in PBS, pH 7.4) and (8) lispro + pramlintide (in PBS, pH 7.4). Zinc(II) was removed from the insulin through competitive binding by the addition of EDTA, which exhibits a dissociation binding constant approaching attomolar concentrations ($K_d \approx 10^{-18}$ M)[40,41]. EDTA was added to the formulations (one equivalent with respect to zinc) to sequester zinc from the formulation. The stability of formulations mixed with CB[7]–PEG were evaluated for: (1) zinc-free aspart (100 U ml^{-1}) + CB[7]–PEG (five equivalents), (2) zinc-free lispro (100 U ml^{-1}) + CB[7]–PEG (five equivalents), (3) pramlintide (in PBS, pH 7) + CB[7]–PEG (five equivalents), (4) zinc-free aspart + pramlintide (pramlintide:insulin molar ratio of 1:20) + CB[7]–PEG (five equivalents), (5) zinc-free lispro + pramlintide (pramlintide:insulin molar ratio of 1:20) + CB[7]–PEG (five equivalents), (6) zinc-free aspart + pramlintide (pramlintide:insulin molar ratio of 1:6) + CB[7]–PEG (five equivalents), (7) zinc-free lispro + pramlintide (pramlintide:insulin molar ratio of 1:6) + CB[7]–PEG (five equivalents), (8) zinc-free lispro + CB[7]–PEG (three equivalents) and (9) zinc-free lispro + pramlintide (pramlintide:insulin molar ratio of 1:6) + CB[7]–PEG (three equivalents).

Streptozotocin (STZ)-induced model of diabetes in rats. Male Sprague Dawley rats (Charles River) were used for the experiments. The animal studies were performed in accordance with the guidelines for the care and use of laboratory animals; all protocols were approved by the Stanford Institutional Animal Care and Use Committee. The protocol used for STZ induction was adapted from the protocol by K. K. Wu and Y. Huan[51]. Briefly, male Sprague Dawley rats (160–230 g; 8–10 weeks) were weighed and fasted 6–8 h before treatment with STZ. The STZ was diluted to 10 mg ml^{-1} in sodium citrate buffer immediately before injection. The STZ solution was injected intraperitoneally to each rat at 65 mg kg^{-1}. The rats were provided with water containing 10% sucrose for 24 h following injection with STZ. The blood glucose levels of the rats were determined daily following STZ treatment to test for hyperglycaemia through tail-vein blood collection using a handheld Bayer Contour Next glucose monitor. Diabetes in non-fasted rats was defined as having three consecutive blood glucose measurements above 400 mg dl^{-1}.

STZ-induced diabetes in swine. Female Yorkshire pigs (Pork Power) were used for the experiments. The animal studies were performed in accordance with the guidelines for the care and use of laboratory animals and all protocols were approved by the Stanford Institutional Animal Care and Use Committee. Type-1-like diabetes was induced in pigs (25–30 kg) using STZ (MedChemExpress). The STZ was infused intravenously at a dose of 125 mg kg^{-1} and the animals were monitored for 24 h. Food and administration of 5% dextrose solution was given as needed to prevent hypoglycaemia. Diabetes was defined as a fasting blood glucose greater than 300 mg dl^{-1}.

In vivo pharmacokinetics and pharmacodynamics in diabetic rats. Diabetic rats were fasted for 6–8 h. The rats were injected subcutaneously with the following formulations: (1) Novolog (1.5 U kg^{-1}), (2) separate injections of Novolog (1.5 U kg^{-1}) and pramlintide, and (3) insulin–pramlintide co-formulation (zinc-free aspart at 1.5 U kg^{-1}; pramlintide at 2.3 μg kg^{-1}) with CB[7]–PEG (five equivalents). For blood glucose measurements, formulations (2) and (3) were evaluated at three different pramlintide-to-aspart ratios: 1:15, 2.3 μg kg^{-1}; 1:8, 4.4 μg kg^{-1}; and 1:2, 17.5 μg kg^{-1}. For the pharmacokinetic studies, only ratios of 1:2 pramlintide to aspart were tested due to the resolution needed for ELISA. The baseline blood glucose levels were measured before injection. Rats with a baseline blood glucose of 400–500 mg dl^{-1} were selected for the study. After injection, blood was sampled every 3 min for the first 30 min, followed by every 5 min for the next 30 min, and then at 75, 90, 120, 150 and 180 min. The blood glucose levels were measured using a handheld blood glucose monitor and additional blood was collected in serum tubes (Starstedt) for analysis with ELISA. The serum pramlintide concentrations were quantified using a human amylin ELISA kit (Phoenix Pharmaceuticals) with pure pramlintide as standards. The serum Novolog concentrations were quantified using a human insulin and insulin analogues ELISA kit (Alpha Diagnostics International) with Novolog standards.

In vivo pharmacokinetics and pharmacodynamics in diabetic swine. Diabetic pigs were fasted for 4–6 h. The pigs were injected subcutaneously with a 4 U dose (0.13 U kg^{-1}) of the following formulations simultaneously with their morning meal (200 g Teklad miniswine diet 8753; 66 g carbohydrates): (1) no treatment (pigs received food only), (2) Humalog (100 U ml^{-1}; Eli Lilly), (3) separate administrations of Humalog and pramlintide (pH 4; 1:6 pramlintide to lispro; 0.5 μg kg^{-1}), (4) lispro–pramlintide co-formulation (zinc-free lispro at 0.13 U kg^{-1}; pramlintide at 0.5 μg kg^{-1}) with CB[7]–PEG (three equivalents to the insulin + pramlintide). Co-formulations with three equivalents CB[7]–PEG were as stable as the current commercial insulin formulations (Supplementary Fig. 9). Insulin lispro was chosen for these studies due to the greater availability of insulin lispro at the time of the experiments and was formulated as previously described[52]. Briefly, EDTA was removed from the formulations using a desalting column and then concentrated to formulate with excipients (phosphate buffer with 2.6% glycerol and 0.85% phenoxyethanol) at 100 U ml^{-1}. Before injection, baseline blood was sampled from an intravenous catheter line and the blood glucose levels were measured using a handheld glucose monitor (Bayer Contour Next). After injection, blood was sampled from the intravenous catheter line every 5 min for the first 60 min and then every 30 min up to 4 h. The blood glucose levels were measured using a handheld blood glucose monitor and additional blood was collected in serum tubes (Starstedt) or K_2EDTA plasma tubes (Greiner-BioOne) for analysis with ELISA. The serum and plasma lispro concentrations were quantified using an iso-insulin ELISA kit or lispro-NL ELISA kit (Mercodia), serum and plasma pramlintide was quantified using a human amylin ELISA kit (Millipore Sigma), and serum and plasma glucagon was quantified using a glucagon ELISA kit (Mercodia). If an ELISA was run multiple times for a sample, the average of the values was used for analysis.

Biocompatibility. Healthy ten-week-old rats ($n = 4$) were administered CB[7]–PEG (0.2 mg kg^{-1}) in PBS (pH 7.4) subcutaneously, once a day for 6 weeks. The experimental dose was equivalent to the CB[7]–PEG concentration in the insulin formulations used for the studies in diabetic rats. Blood was collected for blood chemistry tests on days 14, 28 and 42. Chemistry analysis was performed on a Siemens Dimension Xpand analyzer. A medical technologist performed all of the testing, including dilutions and repeat tests as indicated, and reviewed all of the data. At the end of the 6-week experiment, the rats were euthanized and tissues (kidneys and liver) were collected for histology. The harvested tissue was fixed and transverse sections of the left lateral lobe and right medial lobe of the liver as well as longitudinal sections of the kidney were taken for blinded histological analysis by a professional pathologist ($n = 2$). Haematoxylin and eosin as well as Masson's trichrome staining were performed by Histo-tec Laboratory. Similar to the studies described for rats, diabetic pigs were dosed

with the insulin–pramlintide co-formulation containing CB[7]–PEG at 10–13 meals over the course of 6 weeks. The blood chemistry was analysed as described earlier on blood samples taken 3–4 d following the induction of diabetes and again at the endpoint of the study.

Statistics. All results are expressed as the mean ± s.d. Comparisons between two groups were conducted using a two-tailed Student's *t*-test using GraphPad Prism. Statistical significance was considered at $P < 0.05$. The ROUT method ($Q = 5\%$) or Grubb's method were used to remove outliers when specified.

Reporting Summary. Further information on research design is available in the Nature Research Reporting Summary linked to this article.

Data availability

All data supporting the results in this study are available within the article and its Supplementary information. The broad range of raw datasets acquired and analysed (or any subsets thereof), which would require contextual metadata for reuse, are available from the corresponding author on reasonable request.

Received: 11 October 2018; Accepted: 3 April 2020;
Published online: 11 May 2020

References

1. *Diabetes: Key Facts* (World Health Organization, 2017).
2. Borm, A. K. et al. The effect of pramlintide (amylin analogue) treatment on bone metabolism and bone density in patients with type 1 diabetes mellitus. *Horm. Metab. Res.* **31**, 472–475 (1999).
3. Gottlieb, A. et al. Pramlintide as an adjunct to insulin therapy improved glycemic and weight control in people with type 1 diabetes during treatment for 52 weeks. *Diabetes* **49**, A109 (2000).
4. Ryan, G. J., Jobe, L. J. & Martin, R. Pramlintide in the treatment of type 1 and type 2 diabetes mellitus. *Clin. Ther.* **27**, 1500–1512 (2005).
5. Edelman, S. et al. A double-blind, placebo-controlled trial assessing pramlintide treatment in the setting of intensive insulin therapy in type 1 diabetes. *Diabetes Care* **29**, 2189–2195 (2006).
6. Jones, M. C. Therapies for diabetes: pramlintide and exenatide. *Am. Fam. Physician* **75**, 1831–1835 (2007).
7. Rodriguez, L. M. et al. The role of prandial pramlintide in the treatment of adolescents with type 1 diabetes. *Pediatr. Res.* **62**, 746–749 (2007).
8. Weinzimer, S. A. et al. Effect of pramlintide on prandial glycemic excursions during closed-loop control in adolescents and young adults with type 1 diabetes. *Diabetes Care* **35**, 1994–1999 (2012).
9. Grunberger, G. Novel therapies for the management of type 2 diabetes mellitus: part 1. pramlintide and bromocriptine-QR. *J. Diabetes* **5**, 110–117 (2013).
10. Hay, D. L. et al. Amylin: pharmacology, physiology, and clinical potential. *Pharmacol. Rev.* **67**, 564–600 (2015).
11. Wang, H. et al. Rationally designed, nontoxic, nonamyloidogenic analogues of human islet amyloid polypeptide with improved solubility. *Biochemistry* **53**, 5876–5884 (2014).
12. Ratner, R. et al. Adjunctive therapy with pramlintide lowers HbA1c without concomitant weight gain and increased risk of severe hypoglycemia in patients with type 1 diabetes approaching glycemic targets. *Exp. Clin. Endocrinol. Diabetes* **113**, 199–204 (2005).
13. Whitehouse, F. et al. A randomized study and open-label extension evaluating the long-term efficacy of pramlintide as an adjunct to insulin therapy in type 1 diabetes. *Diabetes Care* **25**, 724–730 (2002).
14. Ratner, R. E. et al. Amylin replacement with pramlintide as an adjunct to insulin therapy improves long-term glycaemic and weight control in type 1 diabetes mellitus: a 1-year, randomized controlled trial. *Diabet. Med.* **21**, 1204–1212 (2004).
15. Hampp, C. et al. Use of antidiabetic drugs in the U.S., 2003–2012. *Diabetes Care* **37**, 1367–1374 (2014).
16. Martin, C. The physiology of amylin and insulin: maintaining the balance between glucose secretion and glucose uptake. *Diabetes Educ.* **32**, 101S–104S (2006).
17. Heptulla, R. A. et al. The role of subcutaneous pramlintide infusion in the treatment of adolescents with type 1 diabetes. *Diabetes* **54**, A110–A111 (2005).
18. Want, L. L. & Ratner, R. Exenatide and pramlintide: new therapies for diabetes. *Int. J. Clin. Pract.* **60**, 1522–1523 (2006).
19. Mathieu, C. et al. Insulin analogues in type 1 diabetes mellitus: getting better all the time. *Nat. Rev. Endocrinol.* **13**, 385–399 (2017).
20. Holleman, F. & Hoekstra, J. B. L. Insulin lispro. *N. Engl. J. Med.* **337**, 176–183 (1997).
21. Gast, K. et al. Rapid-acting and human insulins: hexamer dissociation kinetics upon dilution of the pharmaceutical formulation. *Pharm. Res.* **34**, 2270–2286 (2017).
22. Riddle, M. C. et al. Fixed ratio dosing of pramlintide with regular insulin before a standard meal in patients with type 1 diabetes. *Diabetes Obes. Metab.* **17**, 904–907 (2015).
23. Haidar, A. et al. Insulin-plus-pramlintide artificial pancreas in type 1 diabetes—randomized controlled trial. *Diabetes* **67(Suppl. 1)**, 210-OR (2018).
24. Riddle, M.C. et al. Control of postprandial hyperglycemia in type 1 diabetes by 24-hour fixed-dose coadministration of pramlintide and regular human insulin: a randomized, two-way crossover study. *Diabetes Care* **41**, 2346–2352 (2018).
25. Manning, M. C. et al. Stability of protein pharmaceuticals: an update. *Pharm. Res.* **27**, 544–575 (2010).
26. Mitragotri, S., Burke, P. A. & Langer, R. Overcoming the challenges in administering biopharmaceuticals: formulation and delivery strategies. *Nat. Rev. Drug Discov.* **13**, 655–672 (2014).
27. Yang, C., Lu, D. & Liu, Z. How PEGylation enhances the stability and potency of insulin: a molecular dynamics simulation. *Biochemistry* **50**, 2585–2593 (2011).
28. Guerreiro, L. H. et al. Preparation and characterization of PEGylated amylin. *AAPS PharmSciTech* **14**, 1083–1097 (2013).
29. Sisnande, T. et al. Monoconjugation of human amylin with methylpolyethyleneglycol. *PLoS ONE* **10**, e0138803 (2015).
30. Veronese, F. M. & Mero, A. The impact of PEGylation on biological therapies. *BioDrugs* **22**, 315–329 (2008).
31. Webber, M. J. et al. Supramolecular PEGylation of biopharmaceuticals. *Proc. Natl Acad. Sci. USA* **113**, 14189–14194 (2016).
32. Hirotsu, T. et al. Self-assembly PEGylation retaining activity (SPRA) technology via a host–guest interaction surpassing conventional PEGylation methods of proteins. *Mol. Pharm.* **14**, 368–376 (2017).
33. Bush, M., Bouley, N. & Urbach, A. R. Charge-mediated recognition of N-terminal tryptophan in aqueous solution by a synthetic host. *J. Am. Chem. Soc.* **127**, 14511–14517 (2005).
34. Heitmann, L. M. et al. Sequence-specific recognition and cooperative dimerization of N-terminal aromatic peptides in aqueous solution by a synthetic host. *J. Am. Chem. Soc.* **128**, 12574–12581 (2006).
35. Rajgariah, P. & Urbach, A. R. Scope of amino acid recognition by cucurbit[8] uril. *J. Incl. Phenom. Macro.* **62**, 251–254 (2008).
36. Reczek, J. J. et al. Multivalent recognition of peptides by modular self-assembled receptors. *J. Am. Chem. Soc.* **131**, 2408–2415 (2009).
37. Yin, H. & Wang, R. Applications of cucurbit[*n*]urils ($n = 7$ or 8) in pharmaceutical sciences and complexation of biomolecules. *Isr. J. Chem.* **58**, 188–198 (2018).
38. Walker, S. et al. The potential of cucurbit[n]urils in drug delivery. *Isr. J. Chem.* **51**, 616–624 (2011).
39. Kuok, K. I. et al. Cucurbit[7]uril: an emerging candidate for pharmaceutical excipients. *Ann. NY Acad. Sci.* **1398**, 108–119 (2017).
40. Berthon, G. *Handbook of Metal–Ligand Interactions in Biological Fluids: Bioinorganic Chemistry* (Marcel Dekker, 1995).
41. Waters, R. S. et al. EDTA chelation effects on urinary losses of cadmium, calcium, chromium, cobalt, copper, lead, magnesium, and zinc. *Biol. Trace Elem. Res.* **83**, 207–221 (2001).
42. Hvidt, S. Insulin association in neutral solutions studied by light scattering. *Biophys. Chem.* **39**, 205–213 (1991).
43. Fineberg, S. E. et al. Immunological responses to exogenous insulin. *Endocr. Rev.* **28**, 625–652 (2007).
44. Woods, R. J. et al. Intrinsic fibrillation of fast-acting insulin analogs. *J. Diabetes Sci. Technol.* **6**, 265–276 (2012).
45. da Silva, D. C. et al. Amyloidogenesis of the amylin analogue pramlintide. *Biophys. Chem.* **219**, 1–8 (2016).
46. Like, A. A. & Rossini, A. A. Streptozotocin-induced pancreatic insulitis: new model of diabetes mellitus. *Science* **193**, 415–417 (1976).
47. Gedulin, B. R., Rink, T. J. & Young, A. A. Dose-response for glucagonostatic effect of amylin in rats. *Metabolism* **46**, 67–70 (1997).
48. Knadler, M. P. et al. Addition of 20-kDa PEG to insulin lispro alters absorption and decreases clearance in animals. *Pharm. Res.* **33**, 2920–2929 (2016).
49. Zou, L., Braegelman, A. S. & Webber, M. J. Dynamic supramolecular hydrogels spanning an unprecedented range of host–guest affinity. *ACS Appl. Mater. Interfaces* **11**, 5695–5700 (2019).
50. Chinai, J. M. et al. Molecular recognition of insulin by a synthetic receptor. *J. Am. Chem. Soc.* **133**, 8810–8813 (2011).
51. Wu, K. K. & Huan, Y. Streptozotocin-induced diabetic models in mice and rats. *Curr. Protoc. Pharmacol.* **40**, 5.47.1–5.47.14 (2008).
52. Maikawa, C. L. et al. Stable monomeric insulin formulations enabled by supramolecular PEGylation of insulin analogues. *Adv. Ther.* **3**, 1900094 (2019).

Acknowledgements

This work was funded in part by a NIDDK R01 (the National Institutes of Health grant no. R01DK119254), a Pilot and Feasibility funding from the Stanford Diabetes Research

Center (NIH grant no. P30DK116074) and the Stanford Child Health Research Institute, as well as a Research Starter Grant from the PhRMA Foundation. C.L.M. was supported by the NSERC Postgraduate Scholarship and the Stanford Bio-X Bowes Graduate Student Fellowship. A.A.A.S. was funded by grant no. NNF18OC0030896 from the Novo Nordisk Foundation and the Stanford Bio-X Program, as well as by the Danish Council of Independent Research (grant no. DFF5054-00215). The authors thank the Stanford Animal Diagnostic Lab and the Veterinary Service Centre staff for their technical assistance.

Author contributions

C.L.M., A.A.A.S. and E.A.A. designed experiments and wrote the manuscript. C.L.M., A.A.A.S., L.Z., G.A.R., L.M.S., E.C.G., A.C.Y., J.L.M., S.C., A.K.G., C.M.M., D.C. and C.S.L. performed the experiments. S.W.B. performed the pig surgeries and provided scientific input. C.L.M., A.A.A.S., G.A.R. and M.T. analysed data. D.M.M., B.A.B. and M.J.W. provided scientific input. All authors provided feedback and contributed to writing.

Competing interests

E.A.A., B.A.B., D.M.M., C.L.M. and G.A.R. are inventors on a patent filing (provisional application no. 62/804,357) describing the work reported in this manuscript.

Additional information

Supplementary information is available for this paper at https://doi.org/10.1038/s41551-020-0555-4.

Correspondence and requests for materials should be addressed to E.A.A.

Reprints and permissions information is available at www.nature.com/reprints.

Publisher's note Springer Nature remains neutral with regard to jurisdictional claims in published maps and institutional affiliations.

nature research

Corresponding author(s): Eric Appel

Last updated by author(s): Feb 20, 2020

Reporting Summary

Nature Research wishes to improve the reproducibility of the work that we publish. This form provides structure for consistency and transparency in reporting. For further information on Nature Research policies, see Authors & Referees and the Editorial Policy Checklist.

Statistics

For all statistical analyses, confirm that the following items are present in the figure legend, table legend, main text, or Methods section.

n/a	Confirmed	
☐	☒	The exact sample size (*n*) for each experimental group/condition, given as a discrete number and unit of measurement
☐	☒	A statement on whether measurements were taken from distinct samples or whether the same sample was measured repeatedly
☐	☒	The statistical test(s) used AND whether they are one- or two-sided *Only common tests should be described solely by name; describe more complex techniques in the Methods section.*
☒	☐	A description of all covariates tested
☒	☐	A description of any assumptions or corrections, such as tests of normality and adjustment for multiple comparisons
☐	☒	A full description of the statistical parameters including central tendency (e.g. means) or other basic estimates (e.g. regression coefficient) AND variation (e.g. standard deviation) or associated estimates of uncertainty (e.g. confidence intervals)
☐	☒	For null hypothesis testing, the test statistic (e.g. *F*, *t*, *r*) with confidence intervals, effect sizes, degrees of freedom and *P* value noted *Give P values as exact values whenever suitable.*
☒	☐	For Bayesian analysis, information on the choice of priors and Markov chain Monte Carlo settings
☒	☐	For hierarchical and complex designs, identification of the appropriate level for tests and full reporting of outcomes
☒	☐	Estimates of effect sizes (e.g. Cohen's *d*, Pearson's *r*), indicating how they were calculated

Our web collection on statistics for biologists contains articles on many of the points above.

Software and code

Policy information about availability of computer code

Data collection	No software was used.
Data analysis	GraphPad Prism 6 (GraphPad Software) was used for statistical analysis. All NMR data were processed using MestReNova 11.0.4.

For manuscripts utilizing custom algorithms or software that are central to the research but not yet described in published literature, software must be made available to editors/reviewers. We strongly encourage code deposition in a community repository (e.g. GitHub). See the Nature Research guidelines for submitting code & software for further information.

Data

Policy information about availability of data

All manuscripts must include a data availability statement. This statement should provide the following information, where applicable:

- Accession codes, unique identifiers, or web links for publicly available datasets
- A list of figures that have associated raw data
- A description of any restrictions on data availability

All data supporting the results in this study are available within the Article and its Supplementary Information. The broad range of raw datasets acquired and analysed (or any subsets of it), which for reuse would require contextual metadata, are available from the corresponding author on reasonable request.

Field-specific reporting

Please select the one below that is the best fit for your research. If you are not sure, read the appropriate sections before making your selection.

☒ Life sciences ☐ Behavioural & social sciences ☐ Ecological, evolutionary & environmental sciences

Life sciences study design

All studies must disclose on these points even when the disclosure is negative.

Sample size	Sample size was based on a power calculation using the expected variance and effect sizes.
Data exclusions	The ROUT method (Q = 5%) or Grubbs' method (alpha = 0.05) was used to remove outliers. The ROUT or Grubb's method was selected on the basis of whether there appeared to be one or multiple outliers in a dataset without pre-established exclusion criteria.
Replication	For in vivo studies, the number of samples for a treatment group were divided over two or more different experimental days, and formulations were remade for each rat. Similarly, treatment groups were divided over two or more experimental days for the pig experiments. Formulations came from either 1 or 2 batches per treatment group. Pig experiments were repeated twice with two independent sets of pigs. There were no discernible differences between experimental days or formulations when experiments were repeated, suggesting that replication was successful.
Randomization	Rats were selected arbitrarily to receive different treatments. Each of the pigs received every treatment group, with the order of the treatments given randomly.
Blinding	Histopathology data analysis was performed by a blinded pathologist without knowledge of whether samples were from a control or treatment group. Data for blood glucose and pharmacokinetic experiments in rats and pigs were directly quantifiable, and the analysis was performed blinded.

Reporting for specific materials, systems and methods

We require information from authors about some types of materials, experimental systems and methods used in many studies. Here, indicate whether each material, system or method listed is relevant to your study. If you are not sure if a list item applies to your research, read the appropriate section before selecting a response.

Materials & experimental systems

n/a	Involved in the study
☒	☐ Antibodies
☒	☐ Eukaryotic cell lines
☒	☐ Palaeontology
☐	☒ Animals and other organisms
☒	☐ Human research participants
☒	☐ Clinical data

Methods

n/a	Involved in the study
☒	☐ ChIP-seq
☒	☐ Flow cytometry
☒	☐ MRI-based neuroimaging

Animals and other organisms

Policy information about studies involving animals; ARRIVE guidelines recommended for reporting animal research

Laboratory animals	Sprague Dawley Rat, male, 8–10 weeks of age at the start of the experiment. Yorkshire Pigs, female, 25–30 kg at the start of the experiment.
Wild animals	The study did not involve wild animals.
Field-collected samples	The study did not involve samples collected from the field.
Ethics oversight	The animal studies were performed in accordance with the guidelines for the care and use of laboratory animals, and all protocols were approved by the Stanford Institutional Animal Care and Use Committee.

Note that full information on the approval of the study protocol must also be provided in the manuscript.